J. Anat. (1999) **195**, pp. 419–427 with 7 figures Printed in the United Kingdom

Structural abnormalities do not explain the early functional abnormalities in the peripheral nerves of the streptozotocin diabetic rat

DAVID WALKER[1], ANNE CARRINGTON[2], SUSAN A. CANNAN[2], DIANE SAWICKI[2], JANET SREDY[2], ANDREW J. M. BOULTON[1] AND RAYAZ A. MALIK[1]

[1] *Department of Medicine, Manchester Royal Infirmary, UK and* [2] *The Institute for Diabetes Discovery, Branford, Connecticut, USA*

(*Accepted 25 May 1999*)

ABSTRACT

The streptozotocin (STZ)-diabetic rat, the most commonly employed model of experimental diabetic neuropathy, is characterised by a reduction in nerve conduction velocity, pain threshold and blood flow. Whether or not structural abnormalities underlie these functional abnormalities is unclear. 10 adult male Sprague–Dawley STZ-diabetic rats (diabetes duration 27 d) and 10 age-matched (23 wk) control animals were studied. Motor nerve conduction velocity ($m\ s^{-1}$) was significantly reduced in diabetic (41.31 ± 0.8) compared with control (46.15 ± 1.5) animals ($P < 0.001$). The concentration of sciatic nerve glucose ($P < 0.001$), fructose ($P < 0.001$) and sorbitol ($P < 0.001$) was elevated, and myoinositol ($P < 0.001$) was reduced in diabetic compared with control animals. Detailed morphometric studies demonstrated no significant difference in fascicular area, myelinated fibre density, fibre and axon areas as well as unmyelinated fibre density and diameter. Endoneurial capillary density, basement membrane area and endothelial cell profile number did not differ between diabetic and control animals. However, luminal area ($P < 0.03$) was increased and endothelial cell area ($P < 0.08$) was decreased in the diabetic rats. We conclude there is no detectable structural basis for the reduction in nerve conduction velocity, pain threshold or blood flow, observed in the streptozotocin diabetic rat.

Key words: Diabetes mellitus; peripheral neuropathy; nerve conduction velocity; morphometry; microangiopathy.

INTRODUCTION

Human diabetic polyneuropathy is characterised functionally by a reduction in nerve conduction velocity and action potential amplitude, an increase in sensory thresholds and reduced intraneural oxygen tension with altered nerve blood flow (Boulton & Malik, 1998). These changes are accompanied structurally both by myelinated and unmyelinated nerve fibre degeneration and regeneration (Britland et al. 1990; Llewelyn et al. 1990; Bradley et al. 1995; Malik, 1997) and by endoneurial microangiopathy (Malik et al. 1989, 1992, 1993; Giannini & Dyck, 1995).

Experimental animals have been employed extensively to model human diabetic neuropathy to reproduce nerve conduction velocity deficits, abnormalities of nerve blood flow and altered pain perception thresholds (Kennedy et al. 1982; Sharma et al. 1983; Sharma & Thomas, 1987; Calcutt et al. 1996). Most studies on STZ-diabetic rats, have not demonstrated myelinated fibre loss in a number of peripheral nerves including the sural (Sharma & Thomas, 1974; Brown et al. 1980; Sugimura et al. 1980), tibial (Sharma & Thomas, 1974; Sharma et al. 1981), sciatic (Wright & Nukada, 1994*a*) and peroneal (Jakobson, 1976) nerves. Conflicting reports have arisen on the detailed morphometric changes in myelinated fibre size with some authors finding no abnormalities (Sharma et al. 1981; Wright & Nukada, 1994*a*) and others who report a decrease in fibre size

Correspondence to Dr R. A. Malik, Department of Medicine, Manchester Royal Infirmary, Oxford Road, Manchester M13 , UK. Tel.: +44-161-276-8691; fax: +44-161-274-4740.

(Jakobson, 1976; Bestetti et al. 1981*a*, *b*; Zemp et al. 1981; Thomas et al. 1990; Thomas, 1990). A selective reduction in axonal size in comparison with controls has also been demonstrated in some (Sharma et al. 1983; Sharma & Thomas, 1987; Sima et al. 1987) but not all (Sharma et al. 1980, 1981; Wright & Nukada, 1994*a*; Malone et al. 1996) animal models. Both myelinated and unmyelinated fibre pathology may play a role in altered pain thresholds, however studies on structural abnormalities of the latter group of fibres have again been limited (Sharma & Thomas, 1987). With regard to nerve blood flow, although controversy exists as to whether nerve blood flow is reduced (Cameron et al. 1991) or increased (Williamson et al. 1993) the consensus appears to be for the former. Structural changes in the endoneurial vasculature are not clearly described and require detailed study.

Thus in order to determine the structural changes which may underlie the reduction in nerve conduction velocity, pain threshold and blood flow in the STZ-diabetic rat, we have conducted detailed morphometric studies to quantify nerve fibre and endoneurial capillary pathology, respectively.

MATERIALS AND METHODS

Animals

Ten male Sprague–Dawley rats fasted for 24 h received a single intraperitoneal injection of streptozotocin (Sigma, St Louis, MO) 30 mg/kg body weight in 0.03 M citrate buffer at pH 4.5. Ten control animals received 0.03 M citrate buffer alone. At the time of injection both control and diabetic animals were 19 wk of age with a mean body weight of 450 g. Blood glucose levels and body weights were measured twice weekly and after 27 d motor nerve conduction velocity was measured under isoflurane anaesthesia. The sciatic nerve was then removed and frozen for tissue sugar and polyol estimation and the tibial nerve was harvested and prepared for light and electron microscopy.

Electrophysiology

Motor nerve conduction velocity was measured in the sciatic/tibial-interosseous system employing previously defined methodology (Sharma & Thomas, 1974). The rats were anaesthetised with 4% isoflurane in oxygen (1 l/min) for induction and subsequently 2.5% (control) and 2% (diabetic) (0.5 l/min) for maintenance. Near-nerve temperature was recorded and maintained at 37°C using a wire thermister and thermometer (YSI Tele-thermometer, Model 4000A, Yellow Springs Instrument Co., OH), heat therapy system (Baxter K-MOD 100 pump and DUO Therm pad, Baxter Healthcare, Deerfield, IL) and a source of radiant heat. The left sciatic/tibial nerve was stimulated at the sciatic notch and the Achilles tendon and action potentials were recorded from the interosseous muscle using needle electrodes (Sapphire II, 4ME electrophysiological system, Teca Corp, Pleasantville, NY). The nerve was stimulated by square wave pulses (duration 0.1 ms, intensity 20 V) and the average of 10 action potential traces were measured and the nerve length was measured after dissection. This was repeated 3 times (after removal and replacement of the electrodes) to obtain values for the coefficient of variation.

Biochemistry

Rats were euthanised and cardiac puncture was undertaken to obtain blood for later determination of plasma glucose (hexokinase enzymatic method, Sigma Diagnostica, St Louis, MO) and glycosylated haemoglobin (Glyc-Affin Ghb Kit, Isolab, Akron, OH). Both sciatic nerves were weighed and frozen for polyol estimation by capillary gas chromatography. Frozen tissues were homogenised in cold 5% trichloroacetic acid with Duall tissue grinder, and the deproteinised extracts were analysed as their aldonitrile derivatives.

Nerve biopsy and histology

The distal portion of the tibial nerve was biopsied at a constant site and immediately fixed by immersion in 2.5% glutaraldahyde in 0.2 M sodium cacodylate buffer (pH 7.3). After washing in the same buffer, the nerve was postfixed in 1% cacodylate-buffered osmium tetroxide and following a second wash was dehydrated through ascending concentrations of ethanol before embedding in TAAB Spurr's resin using propylene oxide as an intermediary.

Sections were cut on a Reichert-Jung Ultracut ultramicrotome (Reichert-Jung, Eindhoven, The Netherlands). Semithin (0.75 μm) transverse sections prepared for light microscopy were stained with thionin followed by acridine orange and examined under a Leitz Laborlux SE light microscope (Leitz Wetzler, Germany) with a Leica WILD MPS32 camera attachment (Leica, Heerbrugg, Switzerland).

For electron microscopy, ultrathin (80 nm) transverse sections were transferred to 200-mesh formvar-

Table 1. *Body weight, blood glucose, HbA1c, motor nerve conduction velocity (MNCV) and sciatic nerve polyol levels in control (n = 10) and diabetic (n = 10) animals (mean ± S.E.M.)*

Parameter	Control	Diabetic	*P* value
Body weight (g)	479 ± 5.0	391 ± 8.0	< 0.001
Blood glucose (mmol/l)	4.1 ± 0.2	20.4 ± 1.0	< 0.001
HbA1c (%)	5.1 ± 0.1	13.8 ± 0.4	< 0.001
MNCV (ms^{-1})	46.15 ± 1.5	41.31 ± 0.8	< 0.001
Reproducibility MNCV (CV-%)	2.7 ± 1.6	3.2 ± 1.5	ns
Glucose (nmol/mg)	2.37 ± 0.14	7.43 ± 0.37	< 0.001
Fructose (nmol/mg)	0.87 ± 0.04	6.17 ± 0.41	< 0.001
Sorbitol (nmol/mg)	0.18 ± 0.02	1.32 ± 0.19	< 0.001
Myo-inositol (nmol/mg)	2.49 ± 0.09	1.62 ± 0.06	< 0.001

coated copper grids and contrasted with 2% uranyl acetate in 70% ethanol followed by 0.3% sodium citrate in 0.1 M sodium hydroxide, before viewing in a Philips EM400T transmission electron microscope (Philips, Eindhoven, The Netherlands).

Morphometric procedures

One section/biopsy was chosen from each animal on the basis of optimal preservation and technical quality of staining. Light microscope photomontages of whole nerve fascicles were produced from semithin sections and direct counts were made of the number of myelinated fibres, regenerative clusters (here defined as 2 or more closely apposed small or medium sized myelinated fibres) and endoneurial capillaries. The fascicular area was measured and the density per mm^2 was calculated.

A systematic random sampling technique was employed to obtain electronmicroscope images of the nerve fibres for quantification (Mayhew & Sharma, 1984). The lattice-mesh of the copper support grid provides an ideal basis for sampling. 24 images per sample were taken of myelinated fibres (magnification ×1700) and unmyelinated fibres (magnification ×4600). Myelinated fibres sectioned in the paranodal or perinuclear regions or at Schmidt-Lanterman incisures were excluded and at least 200 fibres per animal were assessed to determine the fibre and axon areas. The density of unmyelinated fibres and Schwann cell profiles was calculated by direct counts from electronmicrographs and the axon diameter was measured employing 2-point digitisation. In addition, 12 images of endoneurial capillaries were taken for each animal at a magnification of ×4600. The luminal, endothelial cell and basement membrane areas were measured and endothelial cell profile number was counted directly. All measurements were made using a hand-held digitiser linked to a microcomputer system (Synoptics, Cambridge).

Statistical analysis

The results are presented as the mean ± S.E.M. Functional and clinical data were assessed for statistical difference using the 2-way ANOVA. All morphometric data were assessed by the Mann–Whitney U test (n = 10 unless otherwise stated).

RESULTS

Clinical observations and electrophysiology

The values for body weight, blood glucose and glycated haemoglobin levels (HbA1c) are shown in Table 1. Prior to biopsy both blood glucose and HbA1c levels were significantly ($P < 0.001$) elevated

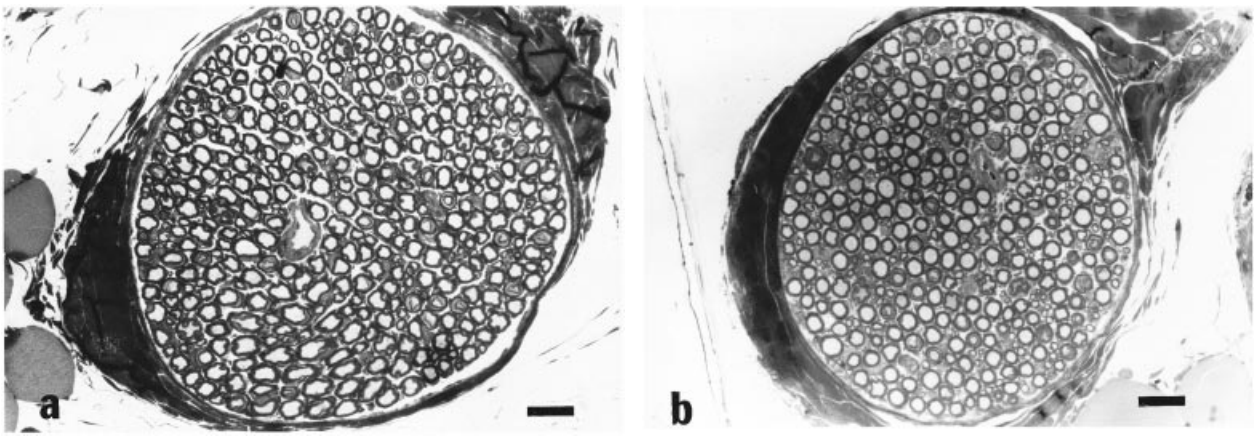

Fig. 1. Light photomicrographs of semithin transverse sections of the tibial nerve from control (*a*) and diabetic (*b*) rats. Bar, 30 μm.

Table 2. *Mean fascicular area* (*FA*), *myelinated fibre density* (*MFd*), *regenerative cluster density* (*RCd*), *fibre and axon area and g ratio plus unmyelinated axon density* (*UAd*), *axon diameter and unassociated Schwann cell profile density* (*USCPd*) *for the tibial nerve of control and diabetic animals* (*mean* ± *S.E.M.*)

Parameter	Control	Diabetic	*P* value
FA (mm^2)	0.19 ± 0.02	0.20 ± 0.03	ns
MFd (no. mm^{-2})	10059 ± 1190	10312 ± 1235	ns
RCd (no. mm^{-2})	71.4 ± 8.7	81.6 ± 11.6	ns
Fibre area (μm^2)	38.6 ± 2.1	38.9 ± 2.4	ns
Axon area (μm^2)	17.9 ± 3.1	17.8 ± 1.5	ns
g ratio	0.46 ± 0.02	0.46 ± 0.03	ns
UAd (no. mm^{-2})	68800 ± 4000	70500 ± 10700	ns
Axon diameter (μm)	0.66 ± 0.01	0.65 ± 0.01	ns
USCPd (%)	10.3 ± 2.1	11.3 ± 2.5	ns

and body weights reduced ($P < 0.001$) in the diabetic compared with control animals. Concentrations of sciatic nerve glucose, fructose and sorbitol were increased ($P < 0.001$) and myo-inositol decreased ($P < 0.001$) in diabetic compared with control animals (Table 1). Motor nerve conduction velocity (MNCV) was significantly reduced ($P < 0.001$) in the diabetic animals compared with control animals (Table 1).

Morphometry

Myelinated fibres. Qualitative (Fig. 1) and quantitative (Table 2) data on myelinated fibres in control and diabetic animals are presented. There was no significant difference in the mean fascicular area and myelinated fibre and regenerative cluster density between diabetic and control animals. Measures of fibre and axon area as well as g ratio were almost identical between the 2 groups. Both myelinated fibre (Fig. 2) and axon (Fig. 3) size distributions were very similar between control and diabetic animals.

Unmyelinated fibres. Qualitative (Fig. 4) and quantitative (Table 2) findings of the unmyelinated axons in the control and diabetic rats are demonstrated. Unmyelinated axon density and the density of Schwann cell profiles show no significant difference between control and diabetic animals. Unassociated Schwann cell profile density and percentage exhibited no difference between the 2 groups. When the number

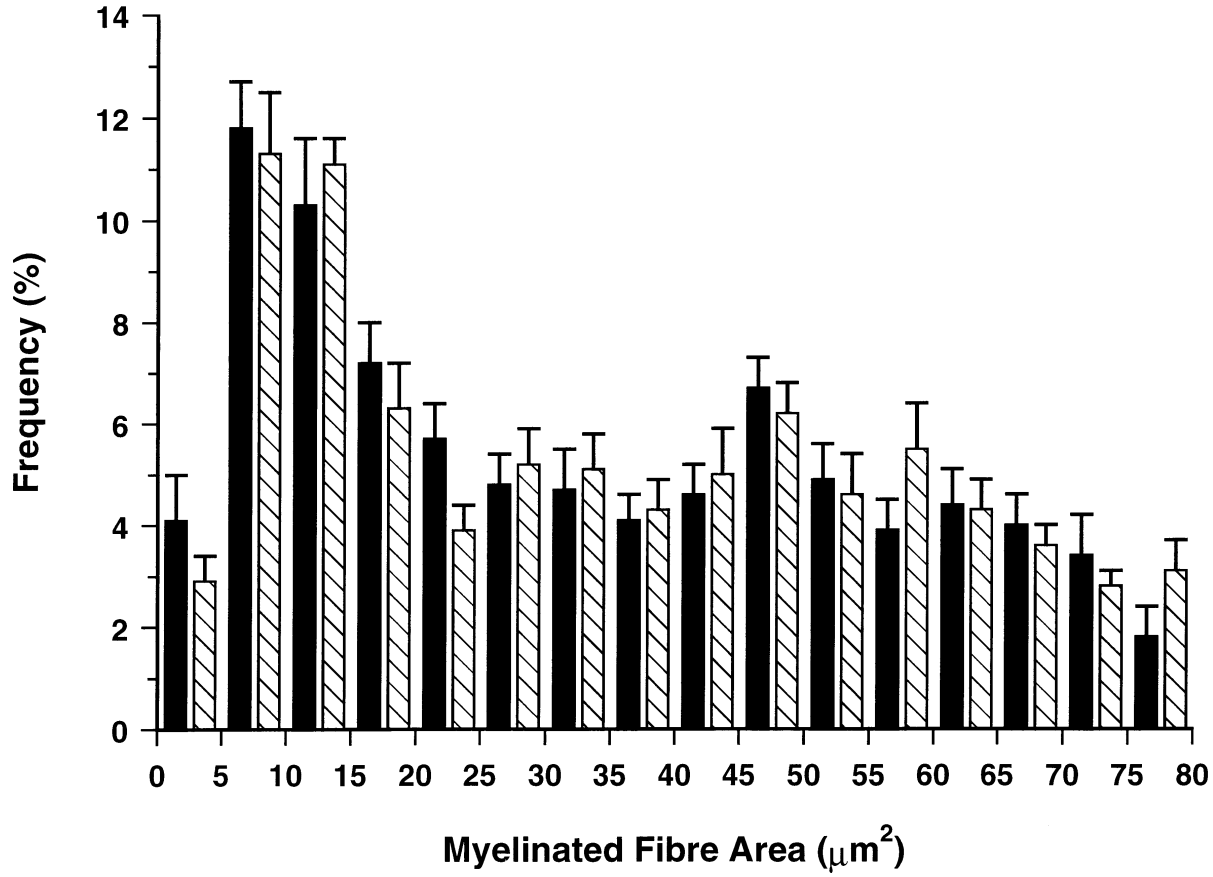

Fig. 2. Myelinated fibre area distribution in control (solid bars) compared with diabetic (hatched bars) rats.

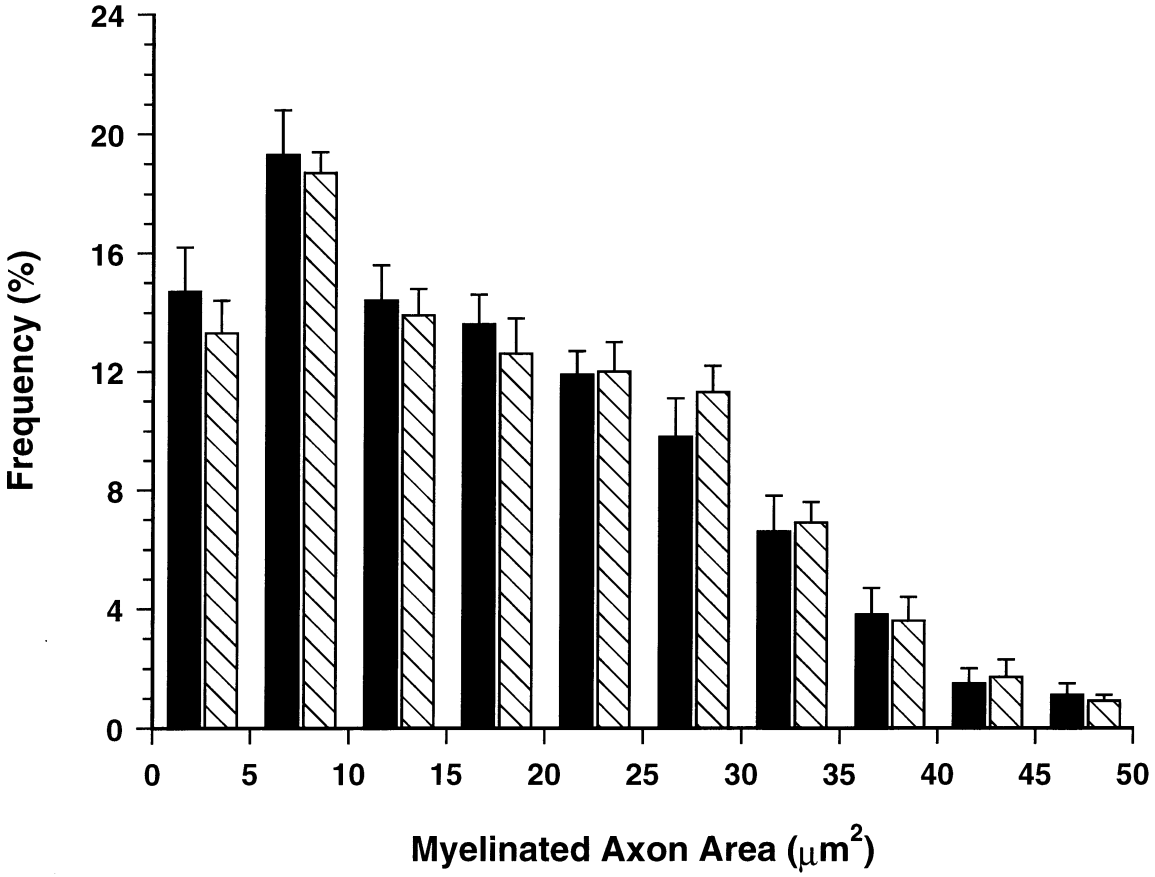

Fig. 3. Myelinated axon area distribution in control (solid bars) compared with diabetic (hatched bars) rats.

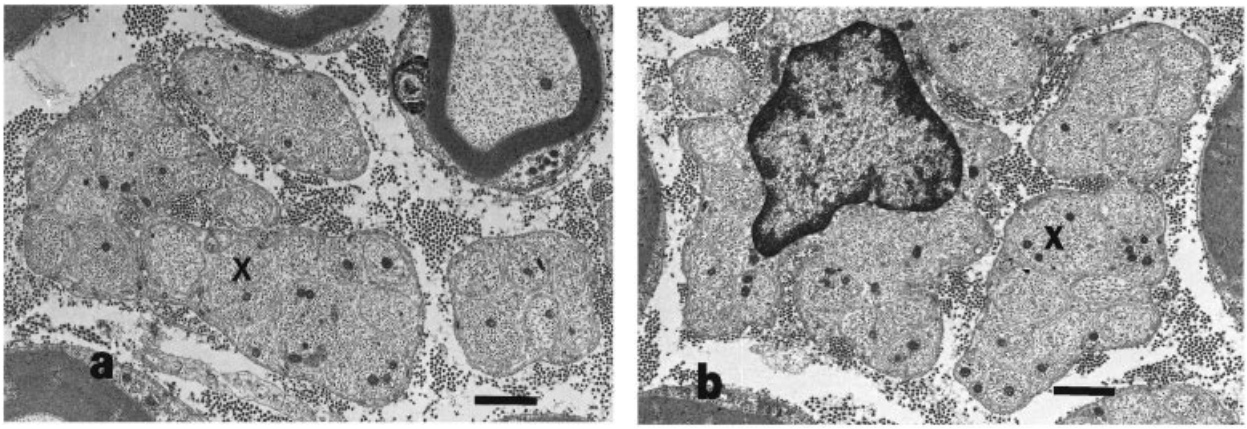

Fig. 4. Electron micrographs of unmyelinated fibres in a control (*a*) and diabetic (*b*) rat, illustrating the qualitative similarity between the 2 groups. X, axon. Bar, 1 μm.

of axons per Schwann cell subunit is plotted against the percentage of Schwann cells (Fig. 5) the resulting distribution histogram is no different in control compared with diabetic animals. No difference is seen in the diameter of the axons in the small fibres between the 2 groups and a similar unimodal size distribution is observed (Fig. 6).

Endoneurial capillaries. Representative electron micrographs of endoneurial capillaries from a control and diabetic rat are shown in Figure 7. The morphometric data for the endoneurial capillaries are shown in Table 3. There was no significant difference in capillary density or endothelial cell profile number between control and diabetic animals. There was no evidence of basement membrane thickening in the diabetic rats. Interestingly, there was a significant increase ($P < 0.03$) in capillary luminal area with a concomitant decrease ($P < 0.08$) in the endothelial

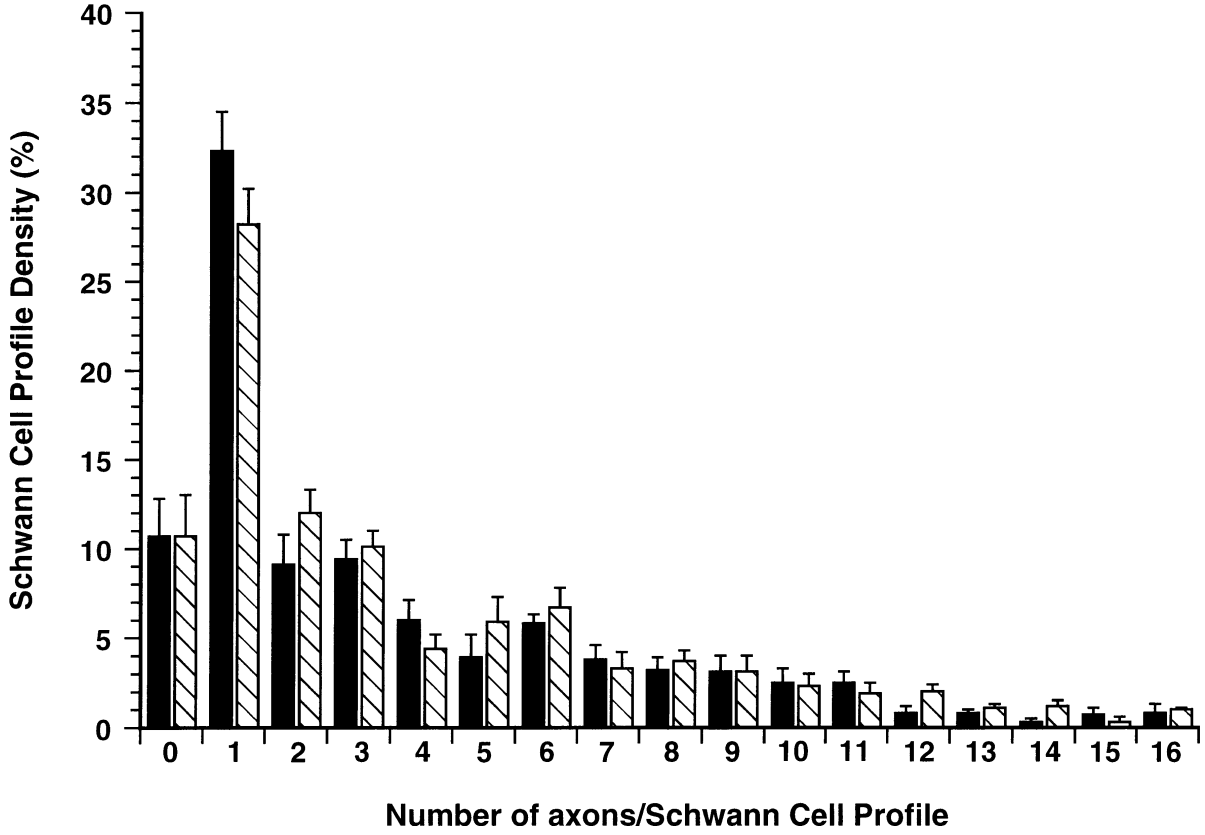

Fig. 5. Percentage distribution of the number of unmyelinated axons per Schwann cell profile in control (solid bars) compared with diabetic (hatched bars) rats.

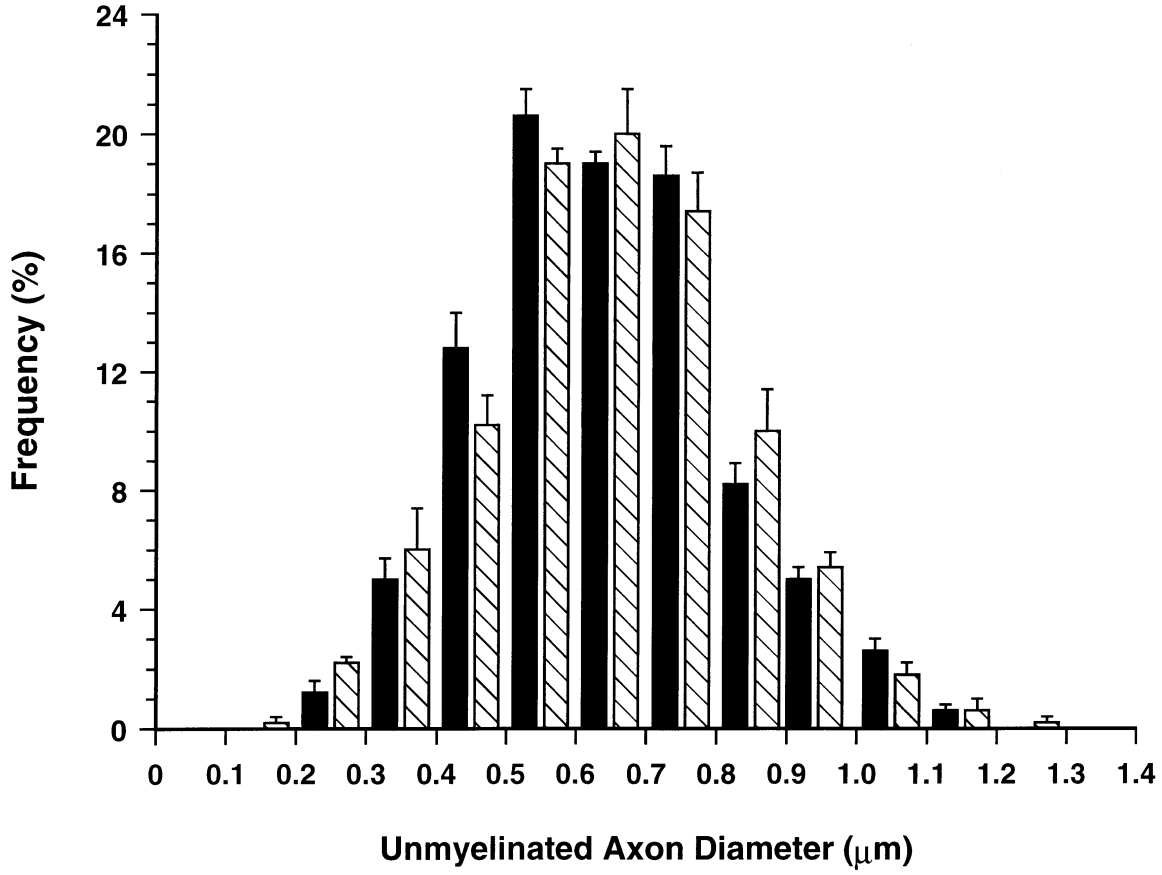

Fig. 6. Unmyelinated axon-size distribution (based on axon diameter) in control (solid bars) compared with diabetic (hatched bars) rats.

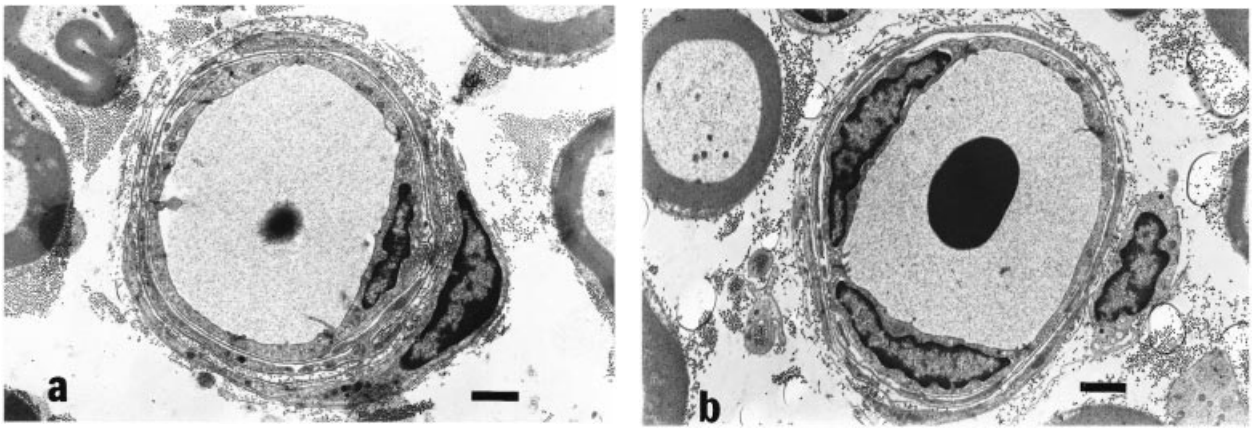

Fig. 7. Electron micrographs of endoneurial capillaries taken from a control (*a*) and diabetic (*b*) rat. Bar, 1.5 μm

Table 3. *Endoneurial capillary density* (*Cd*), *luminal area* (*LA*), *endothelial cell area* (*ECA*), *basement membrane area* (*BMA*) *and endothelial cell profile number* (*ECP no.*) *in the tibial nerve of control and diabetic animals* (*mean* ± *S.E.M.*)

Parameter	Control	Diabetic	*P* value
Cd (no. mm^{-2})	39.1 ± 3.7	41.7 ± 3.0	ns
LA (μm^2)	25.0 ± 2.6	35.4 ± 1.7	< 0.03
ECA (μm^2)	24.8 ± 2.6	21.7 ± 2.6	< 0.08
BMA (μm^2)	16.8 ± 1.1	16.7 ± 2.4	ns
ECP no.	5.3 ± 0.7	5.1 ± 0.3	ns

cell area when comparing diabetic with control animals.

DISCUSSION

The present study has employed detailed light and electron microscopic morphometric techniques to assess the ultrastructure of the tibial nerve in a group of adult STZ-diabetic rats compared with control animals. The diabetic animals demonstrate a significant reduction in motor nerve conduction velocity and also abnormalities of the polyol pathway in keeping with many previous studies in the STZ-diabetic rat (Sharma & Thomas, 1987).

Although experimental animals have been employed extensively to model human diabetic neuropathy, nerve fibre loss and extensive demyelination sufficient to explain the reduction in nerve conduction velocity have not been demonstrated in most animal models (Sharma & Thomas, 1987). This study demonstrates no significant reduction in myelinated fibre density confirming previous studies conducted in the STZ-diabetic rat (Sharma & Thomas, 1987), STZ-diabetic monkey (Chopra et al. 1977), db/db mouse (Sharma et al. 1983), Chinese hamster (Kennedy et al. 1982) and STZ/alloxan-diabetic dog (Walker et al. 1997). Only the BB Wistar rat (Sima et al. 1987) and the spontaneously diabetic dog (Sharma et al. 1995) have demonstrated a distal reduction in myelinated fibre density. Axon diameter has been found to be smaller in diabetic animals than in controls, the difference being greater than for myelin thickness, both in the STZ-diabetic rat (Sharma & Thomas, 1987), and the db/db mouse (Sharma et al. 1983), and axonal atrophy has been claimed in the BB Wistar rat (Sima et al. 1987). The present study did not demonstrate axonal atrophy, in keeping with observations in the Chinese hamster (Kennedy et al. 1982) and the spontaneous (Sharma et al. 1995) and STZ/alloxan-diabetic dog (Walker et al. 1997). Attenuated nerve fibre maturation may explain the reduced axonal size in diabetic rats as nerve fibre diameter continues to increase up until 9–12 months of age. The majority of previously reported studies of the effects of hyperglycaemia on nerve structure have been conducted during this time and some have claimed axonal atrophy. Two recent studies in the STZ-diabetic rat, which have taken nerve maturation into account, have failed to show a reduction in axonal size (Wright & Nukada, 1994*a*; Malone et al. 1996).

Regeneration is a vitally important process necessary to repair damaged nerve. In this study, myelinated fibre regenerative cluster density was no different in diabetic animals compared to controls. Previous studies have demonstrated impaired regeneration in the STZ-diabetic rat, shown by a delay in myelination (Sharma & Thomas, 1975) and axonal regeneration (Longo et al. 1986; Vinik et al. 1995). Limitations of assessing regenerative cluster density employing light microscopy include the inability to detect myelinated fibres that have a very thin myelin sheath. Despite this difficulty, a recent study has employed light mi-

croscopy in sural nerve biopsies from diabetic patients (Bradley et al. 1995) and the results are comparable to previous studies employing electron microscopy (Britland et al. 1990).

Pain is a major clinical problem in diabetic patients and several morphometric studies have demonstrated abnormalities of the unmyelinated fibres in painful neuropathy (Britland et al. 1990; Llewelyn et al. 1990; Malik, 1997). Tactile allodynia and formalin hyperalgesia have been used as indicators of painful neuropathy in the diabetic rat (Calcutt et al. 1996). Few studies have performed a detailed assessment of unmyelinated fibres in experimental diabetes. Of those that have, no morphological abnormalities have been reported in the spontaneously (Sharma et al. 1995) and STZ/alloxan (Walker et al. 1997) diabetic dog, spontaneously diabetic mutant mice (Sharma et al. 1983) or the diabetic rat (Sharma & Thomas, 1974). In this study we demonstrated no major abnormality either in the Schwann cells or axons of unmyelinated fibres in diabetic animals.

Endoneurial capillaries from diabetic patients with neuropathy demonstrate basement membrane thickening, endothelial cell hypertrophy and hyperplasia with pericyte degeneration which relates to neuropathic severity (Malik et al. 1989, 1992, 1993; Giannini & Dyck, 1995). However, patients without evidence of neuropathy display basement membrane thickening and pericyte degeneration only (Giannini & Dyck, 1995). A 50% reduction in sciatic nerve perfusion in the STZ-diabetic rat has been reported from studies using invasive and noninvasive methods including hydrogen clearance microelectrode polarography and laser-Doppler flowmetry, with deficits becoming apparent within 1 wk of diabetes induction (Cameron et al. 1991; Wright & Nukada, 1994*b*). Few previous studies have examined capillary morphology in animal models. In this study, capillary basement membrane area was not significantly increased in diabetic animals. This contrasts with findings in diabetic patients without (Giannini & Dyck, 1995) and with mild (Malik et al. 1992) neuropathy. The STZ-diabetic rat has been reported actually to show a thinner basement membrane than in control animals (Yagihashi et al. 1996). We did not observe endothelial cell hyperplasia. Moreover we demonstrated a significant increase in luminal area and a reduction in endothelial cell size. An increase in luminal size has been demonstrated previously in the STZ-diabetic rat (Yagihashi et al. 1996) and diabetic patients with mild (Malik et al. 1992) and established (Malik et al. 1989) neuropathy. Such an increase in luminal size may suggest an increase in blood flow. Alternatively, it may represent a dilated endoneurial vascular bed due either to an overall reduction in blood flow or increased arteriovenous shunting (Kihara et al. 1994; Tesfaye et al. 1996) which may in turn result in raised back pressure in the endoneurial capillary bed, due to increased flow in the postcapillary epineurial venules.

These detailed morphometric studies demonstrate there is no structural basis for 3 commonly observed functional abnormalities in the STZ-diabetic rat, namely reduced nerve conduction velocity, nerve blood flow and an altered pain threshold. Possible reasons for the lack of pathology in this study may include either the proximal site of biopsy (i.e. the tibial nerve as opposed to the more distal sural) or inadequate duration of diabetes. However, previous studies in the sural nerve (Sharma & Thomas, 1974; Brown et al. 1980; Sugimura et al. 1980) and after prolonged diabetes duration (Sharma & Thomas, 1974; Wright & Nukada, 1994*a*) in the STZ-diabetic rat also report limited morphological abnormalities. Therefore, it seems likely that abnormalities of nerve function in the early stages of diabetes occur due to intrinsic, physiological abnormalities in axonal membrane function (Quasthoff, 1998). Abnormalities of nerve blood flow at this early stage are also likely to be due to functional alterations derived from an alteration in the neurohumoral control of blood flow more proximally (Boulton & Malik, 1998).

REFERENCES

BESTETTI G, ROSSI GL, ZEMP C (1981*a*) Changes in peripheral nerves of rats four months after induction of streptozotocin diabetes. *Acta Neuropathologica* (*Berlin*) **54**, 129–134.

BESTETTI G, ZEMP C, PROBST D, ROSSI GL (1981*b*) Neuropathy and myopathy in the diaphragm of rats after 12 months of streptozotocin-induced diabetes mellitus. A light, electron microscopic and morphometric study. *Acta Neuropathologica* (*Berlin*) **55**, 11–20.

BOULTON AJM, MALIK RA (1998) Diabetic neuropathy. *Medical Clinics of North America* **82**, 909–929.

BRADLEY JL, THOMAS PK, KING RHM, MUDDLE JR, WARD JD, TESFAYE S et al. (1995) Myelinated nerve fibre regeneration in diabetic sensory polyneuropathy: correlation with type of diabetes. *Acta Neuropathologica* (*Berlin*) **90**, 403–410.

BRITLAND ST, YOUNG RJ, SHARMA AK, CLARKE BF (1990) Association of painful and painless diabetic polyneuropathy with different patterns of nerve fibre degeneration and regeneration. *Diabetes* **39**, 898–908.

BROWN MJ, SUMNER AJ, GREENE DA, DIAMOND SM, ASBURY AK (1980) Distal neuropathy in experimental diabetes mellitus. *Annals of Neurology* **8**, 168–178.

CALCUTT NA, JORGE MC, YAKSH TL, CHAPLAN SR (1996) Tactile allodynia and formalin hyperalgesia in streptozotocin-diabetic rats: effects of insulin, aldose reductase inhibition and lidocaine. *Pain* **68**, 293–299.

CAMERON NE, COTTER MA, LOW PA (1991) Nerve blood flow in early experimental diabetes in rats: relation to conduction deficits. *American Journal of Physiology* **261**, E1–E8.

CHOPRA JS, SAWHNEY BB, CHAKRAVORTY RN (1977) Pathology and time relationship of peripheral nerve changes in experimental diabetes. *Journal of the Neurological Sciences* **32**, 53–67.

GIANNINI C, DYCK PJ (1995) Basement membrane reduplication and pericyte degeneration precede development of diabetic polyneuropathy and are associated with its severity. *Annals of Neurology* **37**, 498–504.

JAKOBSON J (1976) Axonal dwindling in early experimental diabetes. I. A study of cross sectioned nerves. *Diabetologia* **12**, 539–546.

KENNEDY WR, QUICK DC, MIYOSHI T, GERRITSEN GC (1982) Peripheral neurology of the diabetic Chinese hamster. *Diabetologia* **23**, 445–452.

KIHARA M, ZOLLMAN PJ, SMITHSON IL, LAGERLUND TD, LOW PA (1994) Hypoxic effect of exogenous insulin on normal and diabetic peripheral nerve. *American Journal of Physiology* **266**, E980–E985.

LLEWELYN JG, GILBY SG, THOMAS PK, KING RHM, MUDDLE JR, WATKINS PJ (1990) Sural nerve morphometry in diabetic autonomic and painful sensory neuropathy. *Brain* **114**, 867–892.

LONGO FM, POWELL HC, LE BEAU J, GERRERO MR, HECKMAN H, MYERS RR (1985) Delayed nerve regeneration in streptozotocin-diabetic rats. *Muscle & Nerve* **9**, 385–393.

MALIK RA (1997) The pathology of human diabetic neuropathy. *Diabetes* **46** (Suppl. 2), S50–S53.

MALIK RA, NEWRICK PG, SHARMA AK, JENNINGS A, AH-SEE AK, MAYHEW TM et al. (1989) Microangiopathy in human diabetic neuropathy: relationship between capillary abnormalities and the severity of neuropathy. *Diabetologia* **32**, 92–102.

MALIK RA, VEVES A, MASSON EA, SHARMA AK, AH-SEE AK, SCHADY W et al. (1992) Endoneurial capillary abnormalities in mild human diabetic neuropathy. *Journal of Neurology, Neurosurgery and Psychiatry* **35**, 557–561.

MALIK RA, TESFAYE S, THOMPSON SD, SHARMA AK, BOULTON AJM, WARD JD (1993) Endoneurial localisation of microvascular damage in human diabetic neuropathy. *Diabetologia* **36**, 454–459.

MALONE JI, LOWITT S, KORTHALS JK, SALEM A, MIRANDA C (1996) The effect of hyperglycemia on nerve conduction and structure is age dependent. *Diabetes* **45**, 209–215.

MAYHEW TM, SHARMA AK (1984) Sampling methods for estimating nerve fibre size. I. Methods for nerve trunks of mixed fascicularity. *Journal of Anatomy* **139**, 45–58.

QUASTHOFF S (1998) The role of axonal ion conductances in diabetic neuropathy: a review. *Muscle & Nerve* **21**, 1246–1255.

SHARMA AK, THOMAS PK (1974) Peripheral nerve structure and function in experimental diabetes. *Journal of the Neurological Sciences* **23**, 1–15.

SHARMA AK, THOMAS PK (1975) Peripheral nerve regeneration in experimental diabetes. *Journal of the Neurological Sciences* 24, 417–424.

SHARMA AK, BAJADA S, THOMAS PK (1980) Age changes in the tibial and plantar nerves of the rat. *Journal of Anatomy* **130**, 417–428.

SHARMA AK, BAJADA S, THOMAS PK (1981) Influence of streptozotocin-induced diabetes on myelinated nerve fibre maturation and on body growth in the rat. *Acta Neuropathologica* (*Berlin*) **53**, 257–265.

SHARMA AK, THOMAS PK, GABRIEL G, STOLINSKI C, DOCKERY P, HOLLINS GW (1983) Peripheral nerve abnormalities in the diabetic mutant mouse. *Diabetes* **32**, 1152–1161.

SHARMA AK, THOMAS PK (1987) Animal models: pathology and pathophysiology. In *Diabetic Neuropathy* (ed. Dyck PJ, Thomas PK, Asbury AK, Winegrad AI, Porte D Jr), pp. 237–252. Philadelphia: W. B. Saunders.

SHARMA AK, MALIK RA, DHAR P, MEHRA RD, AHMED I, LOWRIE CT et al. (1995) Peripheral nerve abnormalities in spontaneously diabetic dog. *International Journal of Diabetes* **3**, 130–139.

SIMA AAF, BRISMAR T, YAGIHASHI S (1987) Neuropathies encountered in the spontaneously diabetic BB Wistar rat. In *Diabetic Neuropathy* (ed. Dyck PJ, Thomas PK, Asbury AK, Winegrad AI, Porte D Jr), pp. 253–265. Philadelphia: W. B. Saunders.

SUGIMURA K, WINDEBANK AJ, NATARAJAN V, LAMBERT EH, SCHMID H, DYCK PJ (1980) Interstitial hyperosmolarity may cause axis cylinder shrinkage in streptozotocin diabetic nerve. *Journal of Neuropathology and Experimental Neurology* **39**, 710–721.

TESFAYE S, MALIK RA, HARRIS N, JAKUBOWSKI J, MODY C, WARD JD (1996) Arterio-venous shunting and proliferating new vessels in acute painful neuropathy of rapid glycaemic control (insulin neuritis). *Diabetologia* **39**, 329–335.

THOMAS PK (1990) The pathogenesis of diabetic neuropathy: current problems and prospects. In *Diabetic Neuropathy* (ed. Ward JD, Goto Y), pp. 3–14. Chichester: Wiley.

THOMAS PK, FRAHER JP, O'LEARY D, MORAN MA, COLE M, KING RHM (1990) Relative growth and maturation of axon size and myelin thickness in the tibial nerve of the rat. 2. Effect of streptozotocin-induced diabetes. *Acta Neuropathologica* (*Berlin*) **79**, 375–386.

VINIK AI, NEWTON PG, LOTTERY TJ, LUIS FJ, DEPT AS, PITTENGER GL et al. (1995) Nerve survival and regeneration in diabetes. *Diabetes Review* **3**, 139–157.

WALKER D, MALIK RA, ANDERSON H, GARDINER TA, BOULTON AJM (1997) The effects of Sulindac on peripheral nerve morphology in the chemically induced diabetic dog. *Diabetologia* **40** (Suppl. 1), A550.

WILLIAMSON JR, CHANG K, FRANGOS M et al., (1993) Hyperglycemic pseudohypoxia and diabetic complications. *Diabetes*, **42**, 801–813.

WRIGHT RA, NUKADA H (1994*a*) Sciatic nerve morphology and morphometry in mature rats with streptozotocin-induced diabetes. *Acta Neuropathologica* (*Berlin*) **88**, 571–578.

WRIGHT RA, NUKADA H (1994*b*) Vascular and metabolic factors in the pathogenesis of experimental diabetic neuropathy in mature rats. *Brain* **117**, 1395–1407.

YAGIHASHI S, SUGIMOTO K, WADA R (1996) Endoneurial vessel abnormalities in diabetic animal models. In *Lessons from Animal Diabetes VI* (ed. Shafrir E, pp. 375–393). Boston: Birkhauser.

ZEMP C, BESTETTI G, ROSSI GL (1981) Morphological and morphometric study of peripheral nerves from rats with streptozotocin–induced diabetes mellitus. *Acta Neuropathologica* (*Berlin*) **53**, 99–106